Video Article

# Characterization of Immune Cell-derived Extracellular Vesicles and Studying Functional Impact on Cell Environment

Quentin Lemaire[1], Marie Duhamel[1], Antonella Raffo-Romero[1], Michel Salzet[1], Christophe Lefebvre[1]

[1]U1192-Laboratoire Protéomique, Réponse Inflammatoire et Spectrométrie de Masse (PRISM), Univ. Lille, INSERM

Correspondence to: Christophe Lefebvre at christophe.lefebvre@univ-lille.fr

URL: https://www.jove.com/video/60118
DOI: doi:10.3791/60118

Keywords: Neuroscience, Issue 160, Immune functions, microglia, macrophages, neurons, glioma cells, extracellular vesicles

Date Published: 6/2/2020

Citation: Lemaire, Q., Duhamel, M., Raffo-Romero, A., Salzet, M., Lefebvre, C. Characterization of Immune Cell-derived Extracellular Vesicles and Studying Functional Impact on Cell Environment. *J. Vis. Exp.* (160), e60118, doi:10.3791/60118 (2020).

## Abstract

The neuroinflammatory state of the central nervous system (CNS) plays a key role in physiological and pathological conditions. Microglia, the resident immune cells in the brain, and sometimes the infiltrating bone marrow-derived macrophages (BMDMs), regulate the inflammatory profile of their microenvironment in the CNS. It is now accepted that the extracellular vesicle (EV) populations from immune cells act as immune mediators. Thus, their collection and isolation are important to identify their contents but also evaluate their biological effects on recipient cells. The present data highlight chronological requirements for EV isolation from microglia cells or blood macrophages including the ultracentrifugation and size-exclusion chromatography (SEC) steps. A non-targeted proteomic analysis permitted the validation of protein signatures as EV markers and characterized the biologically active EV contents. Microglia-derived EVs were also functionally used on primary culture of neurons to assess their importance as immune mediators in the neurite outgrowth. The results showed that microglia-derived EVs contribute to facilitate the neurite outgrowth in vitro. In parallel, blood macrophage-derived EVs were functionally used as immune mediators in spheroid cultures of C6 glioma cells, the results showing that these EVs control the glioma cell invasion in vitro. This report highlights the possibility to evaluate the EV-mediated immune cell functions but also understand the molecular bases of such a communication. This deciphering could promote the use of natural vesicles and/or the in vitro preparation of therapeutic vesicles in order to mimic immune properties in the microenvironment of CNS pathologies.

## Video Link

The video component of this article can be found at https://www.jove.com/video/60118/

## Introduction

Many neuropathologies are related to the neuro-inflammatory state which is a complex mechanism that is increasingly considered, but still poorly understood because the immune processes are diverse and depend upon the cell environment. Indeed, the CNS disorders do not systematically involve the same activation signals and immune cell populations and thus the pro- or anti-inflammatory responses are difficult to evaluate as causes or consequences of pathologies. The brain resident macrophages called “microglia” appear to be at the interface between the nervous and immune systems[1]. Microglia have a myeloid origin and are derived from the yolk sac during primitive hematopoiesis to colonize the brain, whereas peripheral macrophages are derived from the fetal liver during definitive hematopoiesis to become peripheral macrophages[2]. The microglia cells communicate with neurons and neuron-derived glial cells such as astrocytes and oligodendrocytes[3]. Several recent studies have demonstrated that microglia are involved in neuronal plasticity during CNS development and adult tissue homeostasis, and also in the inflammatory state associated with neurodegenerative diseases[4,5]. Otherwise, the integrity of the blood brain barrier can be compromised in other CNS pathologies. The immune responses, especially in the glioblastoma multiforme cancer, are not supported only by microglia cells as the blood brain barrier is reorganized through angiogenic processes and the presence of lymphatic vessels[6,7]. Therefore, a large bone marrow-derived macrophages (BMDMs) infiltration occurs in the brain tumor throughout tumor-dependent angiogenesis mechanisms[8]. The cancer cells exert a significant influence on infiltrated BMDMs leading to immunosuppressive properties and tumor growth[9]. Thus the communication between the immune cells and their brain microenvironment is difficult to understand as the cell origin and activation signals are diverse[10,11]. It is thus interesting to apprehend the functions of immune cell-associated molecular signatures in physiological conditions. In this regard, the cell-cell communication between immune cells and cell microenvironment can be studied through the release of extracellular vesicles (EVs).

The EVs are being studied more and more in the regulation of immune functions in healthy as well as pathological conditions[12,13]. Two populations, exosomes and microvesicles, can be taken into account. They present different biogenesis and size ranges. The exosomes are vesicles of ~30–150 nm diameter and are generated from the endosomal system and secreted during fusion of multivesicular bodies (MVBs) with the plasma membrane. The microvesicles are about 100–1,000 nm in diameter and are generated by an outward budding from the cell plasma membrane[14]. Because the exosome versus microvesicle discrimination is still difficult to realize according to the size and molecular patterns, we will only use the term EVs in the present report. The EV-associated communication in the CNS represents an ancestral mechanism since studies showed their involvement in invertebrate species including nematodes, insects or annelids[15,16]. Moreover, the results showing that EVs can communicate with cells from different species demonstrate this mechanism to be a key-lock system, based first on surface-molecule recognition between vesicles and recipient cells and then allowing the uptake of mediators[16,17]. Indeed, the EVs contain many molecules like proteins (e.g., enzymes, signal transduction, biogenesis factor), lipids (e.g., ceramide, cholesterol) or nucleic acids (e.g., DNA, mRNA or miRNAs) acting as

 

direct or indirect regulators of the recipient cell activities[14]. That is why methodological studies were also performed on immune cells to isolate EVs and fully characterize their protein signatures[18,19].

The earliest studies demonstrated the release of exosomes from primary cultured rat microglia as an inducible mechanism following a Wnt3a- or serotonin-dependent activation[20,21]. Functionally in the CNS, microglia-derived EVs regulate the synaptic vesicle release by presynaptic terminals in neurons contributing to the control of the neuronal excitability[22,23]. Microglia-derived EVs could also propagate cytokines-mediated inflammatory response in large brain regions[24,25]. Importantly, the diverse ligands for toll-like receptor family might activate specific productions of EVs in the microglia[26]. For example, in vitro studies show that LPS-activated microglia BV2 cell lines produce differential EV contents including pro-inflammatory cytokines[27]. Therefore, the functional diversity of immune cell subpopulations in the CNS, microglia and infiltrating BMDMs, might be evaluated through their own EV populations including the EV impact on recipient cells and the identification of EV contents.

We previously described methods to evaluate the functional properties of microglia- and BMDM-derived EVs after their isolation[16,19]. In the present report, we propose to independently evaluate the effect of microglia-derived EVs on neurite outgrowth, and the effect of macrophage-derived EVs on the control of glioma cell aggregates. This study also proposes a wide proteomic analysis of the EV fractions in order to validate the EV isolation procedure as well as identify the biologically active protein signatures. The beneficial effects and the molecular deciphering of EV contents could help their possible manipulation and use as therapeutic agents in brain disorders.

## Protocol

# 1. Primary Culture of Microglia/Macrophages

1. **Primary culture of microglia**
    1. Culture commercial rat primary microglia (2 x $10^6$ cells) (see the **Table of Materials**) in Dulbecco's modified Eagle medium (DMEM) supplemented with 10% exosome-free serum, 100 U/mL of penicillin, 100 µg/mL streptomycin, and 9.0 g/L glucose at 37 °C and 5% $CO_2$.
    2. Collect the conditioned medium after a 48 h culture and proceed to the isolation of EVs.
2. **Primary culture of macrophages**
    1. Culture commercial rat primary macrophages (1 x $10^6$ cells) in the medium provided by the manufacturer (see the **Table of Materials**) at 37 °C and 5% $CO_2$, with exosome-free serum.
    2. Collect the conditioned medium after a 24 h culture and proceed to the isolation of EVs.

# 2. Isolation of EVs

1. **Pre-isolation of EVs from conditioned medium**
    1. Transfer the conditioned culture medium from microglia or macrophage cultures (steps 1.1.2 or 1.2.2) into a conical tube.
    2. Centrifuge at 1,200 x *g* for 10 min at room temperature (RT) to pellet the cells.
    3. Transfer the supernatant into a new conical tube. Centrifuge at 1,200 x *g* for 20 min at RT to eliminate apoptotic bodies.
    4. Transfer the supernatant into a 10.4 mL polycarbonate tube and transfer the tube into a 70.1 Ti rotor. Ultracentrifuge at 100,000 x *g* for 90 min at 4 °C to pellet the EVs.
    5. Discard the supernatant and resuspend the pellet containing EVs in 200 µL of 0.20 µm filtered phosphate buffer saline (PBS).
2. **Isolation of EVs**
    1. Preparation of the home-made size exclusion chromatography column (SEC)
        1. Empty a glass chromatography column (length: 26 cm; diameter: 0.6 cm) (see the **Table of Materials**), wash and sterilize it.
        2. Place a 60 µm filter at the bottom of the column.
        3. Stack the column with cross-linked agarose gel filtration base matrix to create a stationary phase of a 0.6 cm diameter and a 20 cm height.
        4. Rinse the phase with 50 mL of 0.20 µm filtered PBS. Store at 4 °C to be used later if necessary.
    2. Place the resuspended EV pellet on top of the stationary phase of the SEC column.
    3. Collect 20 sequential fractions of 250 µL while continuing to add 0.20 µm filtered PBS on the top of stationary phase to prevent drying of the column. Store the fractions at -20 °C if necessary.
    **NOTE:** A longer storage than one week can be performed at -80 °C to maintain the EV integrity for molecular analysis.
3. **Matrix assisted laser desorption ionization (MALDI) mass spectrometry analysis of the SEC fractions**
    1. Proceed to the EV isolation as described in section 2.2.
    2. Resuspend the EV pellet with 200 µL of peptide calibration mix solution (see the **Table of Materials**).
    3. Proceed to EV collection as described in sections 2.2.1 to 2.2.3.
    4. Completely dry the fraction with a vacuum concentrator.
    5. Reconstitute the fractions with 10 µL of 0.1% trifluoroacetic acid (TFA).
    6. Mix 1 µL of reconstituted fraction with 1 µL of α-cyano-4-hydroxycinnamic acid (HCCA) matrix on a MALDI polished steel target plate.
    7. Analyze all fractions with a MALDI mass spectrometer.
    8. Analyze generated spectra with dedicated software (see **Table of Materials**).

## 3. Characterization of EVs

1. **Nanoparticle tracking analysis (NTA)**
   **NOTE:** The NTA analysis is performed with a nanoparticle tracking analysis instrument (see the **Table of Materials**) and an automated syringe pump.
   1. Make a dilution (range of 1:50 to 1:500) of each SEC fraction from step 2.2.3 with 0.20 µm filtered PBS.
   2. Vortex the solution to eliminate EV aggregates.
   3. Put the diluted solution in a 1 mL syringe and place it in the automated syringe pump.
   4. Adjust **Camera setting** to screen gain level (3) and camera level (13).
   5. Click on **Run** and launch the following script.
      1. Load the sample in analysis chamber (infusion rate: 1,000 for 15 s).
      2. Decrease and stabilize speed flow for video recording (infusion rate: 25 for 15 s). Capture three consecutive 60 s videos of the particle flow.
      3. Adjust the camera level (13) and the detection threshold (3) before videos analysis. Click on **Settings| Ok** to start the analysis and click on **Export** when the analysis is done.
   6. Between each fraction analysis, wash with 1 mL of 0.20 µm filtered PBS.

2. **Electron microscopy (EM) analysis**
   1. Isolate EVs as described in section 2.
      **NOTE:** Sterile conditions are not required.
   2. Repeat section 3.1 to quantify EVs.
      **NOTE:** Only positive fractions will be used for EM analysis.
   3. Use a 50 kDa centrifugal filter (see **Table of Materials**) to concentrate EV-containing SEC fractions.
   4. Resuspend concentrated EVs in 30 µL of 2% paraformaldehyde (PFA).
   5. Load 10 µL of the sample onto a carbon-coated copper grid.
   6. Incubate for 20 min in a wet environment.
   7. Repeat steps 3.2.5 and 3.2.6 for a good absorption of the sample on the grid.
   8. Transfer the grid into a drop of 1% glutaraldehyde in PBS for 5 min at RT.
   9. Wash the sample with ultrapure water several times.
   10. Contrast the sample for 10 min on ice with a mixture of 4% uranyl acetate and 2% methylcellulose (1:9, v/v). Remove excess of the mixture using a filter paper.
   11. Dry the sample and observe it under a transmission electron microscope at 200 kV (see the **Table of Materials**).

3. **Western blot analysis**
   1. Protein extraction
      1. Repeat the steps 3.2.1 to 3.2.3 to isolate and concentrate EVs.
      2. Mix 50 µL of RIPA buffer (150 mM sodium chloride [NaCl], 50 mM Tris, 5 mM Ethylene glycol-bis(2-aminoethylether)-N,N,N′,N′-tetraacetic acid [EGTA], 2 mM Ethylenediamine-tetraacetic acid [EDTA], 100 mM sodium fluoride [NaF], 10 mM sodium pyrophosphate, 1% Nonidet P-40, 1 mM Phenylmethanesulfonyl fluoride [PMSF], 1x protease inhibitor) with the EV sample (25 µL resulting from the EV concentration on filter) for 5 min on ice to extract proteins.
      3. Sonicate for 5 s (amplitude: 500 W; frequency: 20 kHz), 3 times on ice.
      4. Remove vesicular debris by centrifugation at 20,000 x *g* for 10 min, at 4 °C.
      5. Collect the supernatant and measure the protein concentration with Bradford protein assay method.
   2. Sodium dodecyl sulfate polyacrylamide gel electrophoresis (SDS-PAGE) and western blotting
      1. Mix protein extracts (30 µg) with 5c Laemmli sample buffer (v/v).
      2. Load the protein mix on a 12% polyacrylamide gel.
      3. Migrate the proteins in the gel with TGS buffer (25 mM Tris pH 8.5, 192 mM Glycine, and 0.1% SDS), at 70 V for 15 min and 120 V for 45 min.
      4. Transfer the proteins onto nitrocellulose membrane with semi-dry system at 230 V for 30 min.
      5. Saturate the membrane for 1 h at RT with blocking buffer (0.05% Tween 20 w/v, 5% milk powder w/v in 0.1 M PBS, pH 7.4).
      6. Incubate the membrane overnight at 4 °C with mouse monoclonal anti-human heat-shock protein 90 (HSP90) antibody diluted in blocking buffer (1:100).
      7. Wash the membrane three times with PBS-Tween (PBS, 0.05% Tween 20 w/v) for 15 min.
      8. Incubate the membrane for 1 h at RT with goat horseradish peroxidase-conjugated anti-mouse IgG secondary antibody diluted in blocking buffer (1:10,000).
         **NOTE:** A negative control is performed using secondary antibody alone.
      9. Repeat the washing step (step 3.3.2.7).
      10. Reveal the membrane with enhanced chemiluminescence (ECL) western blotting substrate kit (see **Table of Materials**).

4. **Proteomic analysis**
   1. Protein extraction and in-gel digestion
      1. Repeat the steps 3.2.1 to 3.2.3 to isolate and concentrate the EVs. Repeat step 3.3.1 for EV protein extraction.
      2. Perform protein migration in the stacking gel of a 12% polyacrylamide gel.
      3. Fix the proteins in the gel with coomassie blue for 20 min at RT.
      4. Excise each colored gel piece and cut it into small pieces of 1 $mm^3$.

5. Wash the gel pieces successively with 300 µL of each solutions: ultrapure water for 15 min, 100% acetonitrile (ACN) for 15 min, 100 mM ammonium bicarbonate ($NH_4HCO_3$) for 15 min, ACN:100 mM $NH_4HCO_3$ (1:1, v/v) for 15 min, and 100% ACN for 5 min with continuous stirring.
6. Dry completely gel pieces with vacuum concentrator.
7. Perform protein reduction with 100 µL of 100 mM $NH_4HCO_3$ containing 10 mM dithiothreitol for 1 h at 56°C.
8. Perform protein alkylation with 100 µL of 100 mM $NH_4HCO_3$ containing 50 mM iodoacetamide for 45 min in the dark at RT.
9. Wash the gel pieces successively with 300 µL of each solution: 100 mM of $NH_4HCO_3$ for 15 min, ACN:20 mM $NH_4HCO_3$ (1:1, v/v) for 15 min, and 100% ACN for 5 min with a continuous stirring.
10. Completely dry the gel pieces with a vacuum concentrator.
11. Perform protein digestion with 50 µL of trypsin (12.5 µg/mL) in 20 mM $NH_4HCO_3$ overnight at 37 °C.
12. Extract the digested proteins from the gel with 50 µL of 100% ACN for 30 min at 37 °C and then 15 min at RT with continuous stirring.
13. Repeat the following extraction procedures twice: 50 µL of 5% TFA in 20 mM $NH_4HCO_3$ solution for 20 min with continuous stirring.
14. Add 100 µL of 100% ACN for 10 min with continuous stirring.
15. Dry digested proteins with a vacuum concentrator and resuspend in 20 µL of 0.1% TFA.
16. Desalt the sample using a 10 µL pipette tip with C18 reverse phase media for desalting and concentrating peptides (see the **Table of Materials**) and elute peptides with ACN:0.1% formic acid (FA) (80:20, v/v).
17. Completely dry the sample with a vacuum concentrator and resuspend in 20 µL of ACN:0.1% FA (2:98, v/v) for liquid chromatography tandem mass spectrometry (LC-MS/MS).

2. LC-MS/MS Analysis
    1. Load the digested peptide into the LC-MS/MS instrument and perform sample and data analysis according to parameters described in detail elsewhere[42].

3. Raw data analysis
    1. Process mass spectrometry data to identify proteins and compare identified proteins of each sample with a quantitative proteomics software package using standard parameters.
    2. Export, using standard parameters, the list of exclusive and over-represented proteins from EV positive samples in a software predicting protein networks and biological processes.
    3. Compare the list of identified proteins in the fractions with the top 100 EV markers from the Exocarta open access database (see the **Table of Materials**).

## 4. Functional EVs Effects Assay

1. **Neurite outgrowth assay on PC-12 cell line**
    1. Culture PC12 cell line in complete DMEM medium (2 mM L-glutamine, 10% fetal horse serum (FHS), 5% fetal bovine serum (FBS), 100 UI/mL penicillin, 100 µg/mL streptomycin).
    **NOTE:** The sera are exosome free in the whole procedure.
    2. Add a cover glass (all wells) to a 24-well plate; coat the plate with poly-D-lysine (0.1 mg/mL) and seed 260,000 cells/well.
    3. Incubate the cells at 37 °C under 5% $CO_2$.
    4. After 24 h of incubation, change the medium to DMEM differentiation medium (DMEM with 2 mM L-glutamine, 0.1% FHS, 100 UI/mL penicillin, 100 µg/mL streptomycin) with 1 x $10^6$ microglia EVs (from step 1.1.2).
    **NOTE:** Control condition is performed without microglia EVs in the differentiation medium.
    5. At day 4 after seeding, load all wells with 100 µL of complete DMEM medium.
    6. At day 7 after seeding, fix the cells with 4% PFA for 20 min at RT and rinse three times (10 min each) with PBS.
    7. Stain the cells with rhodamine-conjugated phalloidin for 30 min at 4 °C and rinse 3 times (10 min each) with PBS.
    8. Stain the cells with diluted Hoechst 33342 (1:10,000) for 30 min at RT and rinse 3 times (10 min each) with PBS.
    9. Mount the cover glass on a slide with fluorescent mounting medium (see **Table of Materials**).
    10. Analyze the slide with a confocal microscope, take 5 random images of each slide.
    11. Measure neurite outgrowth using an automated quantification software (total neurite length) as described in detail elsewhere[43].

2. **Neurite outgrowth on rat primary neurons**
    1. Coat an 8-well glass slide with poly-D-lysine (0.1 mg/mL) and laminin (20 µg/mL).
    2. Culture rat commercial primary neurons in appropriate culture medium (see **Table of Materials**) by plating 50,000 cells per well and incubating the cells at 37 °C under 5% $CO_2$ for 48 h.
    **NOTE:** The sera are exosome-free in the whole procedure.
    3. Add 1 x $10^6$ microglia EVs to neuron culture medium and incubate at 37 °C under 5% $CO_2$ for 48 h more.
    **NOTE:** Control condition is performed without microglia EVs in neuron culture medium.
    4. Follow steps 4.1.6 to 4.1.9 to fix and stain the cells.
    5. Follow steps 4.1.10 and 4.1.11 to analyze the slide.

3. **Glioma cell invasion**
    1. Resuspend C6 rat glioma cells in complete DMEM medium (DMEM with 10% FBS, 2 mM L-glutamine, 1x antibiotics) containing 5% collagen at a final concentration of 8,000 cells in 20 µL.
    **NOTE:** The sera are exosome-free in the whole procedure.
    2. Place 5 mL of PBS AT the bottom of a 60 mm tissue culture dish. Invert the lid and deposit drops of 20 µL (8,000 cells) of cell suspension onto the bottom of the lid.

3. Invert the lid onto the PBS-filled bottom chamber and incubate the plate at 37 °C and 5% $CO_2$ for 72 h until cell spheroids are formed.
4. Add 1 x $10^8$ macrophage EVs (from step 1.2.2) to a 2.2 mg/mL collagen mixture (2 mL of bovine collagen type I solution [3 mg/mL] with 250 µL of 10x minimum essential medium (MEM) and 500 µL of 0.1 M sodium hydroxide).
   **NOTE:** Control condition is performed without macrophage EVs in the collagen mixture.
5. Distribute the collagen mixture containing EVs in a 24-well plate for embedding cell spheroids.
6. Implant the newly formed cell spheroids at the center of each well.
7. Incubate the plate for 30 min at 37°C and 5% $CO_2$ to solidify the gel.
8. Thereafter, overlay 400 µL of complete DMEM medium on the collagen matrix in each well.
9. Incubate the complete system for a total of 6 days at 37 °C and 5% $CO_2$.
   **NOTE:** Cell invasion out of the spheroid is monitored by digital photography using an inverted light microscope using a 4x/0.10 N.A. objective.
10. Acquire images of each well every day.
11. Process images and quantify invasion of cell spheroid areas using the software as previously described in detail[42].
    **NOTE:** Invasion and spheroid areas were normalized for each day to the invasion and spheroid areas measured on day 0.

## Representative Results

One of the main challenges to attributing biologicals effects to extracellular vesicles (EVs) is the ability to isolate the EVs from the whole culture medium. In this report, we present a method using ultracentrifugation (UC) and size-exclusion chromatography (SEC) which is coupled to the large-scale analysis of protein signatures to validate EV markers and identify bioactive compounds. The macrophage- or microglia-derived EVs were isolated from the conditioned medium after a 24 h or 48 h culture respectively (**Figure 1**).

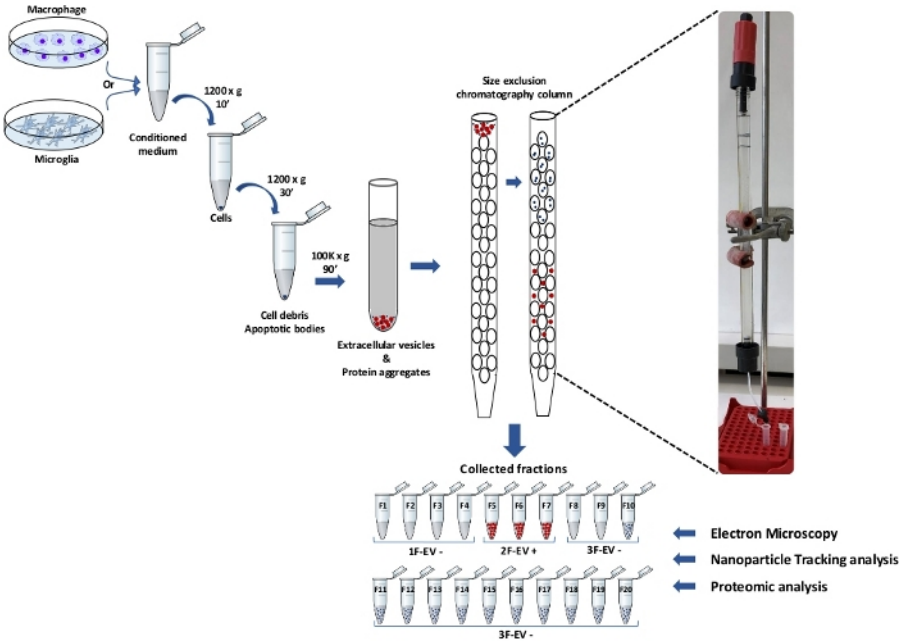


**Figure 1: Extracellular Vesicle (EV) collection and isolation strategies.** The apoptotic bodies and the cell debris were separated from the microglia- or macrophage-conditioned medium by successive centrifugation steps. From the supernatant, EVs were isolated by ultracentrifugation (UC). The UC pellet containing EVs was loaded onto column and separated by size-exclusion chromatography (SEC) in 20 different eluted fractions. As revealed in the further steps (electron microscopy, nanoparticle tracking analysis and proteomic analysis), the SEC fractions were pooled and organized into 1F-EV-, 2F-EV+ and 3F-EV-. Please click here to view a larger version of this figure.

The method followed successive centrifugation steps: the first to remove the cells and the second to remove cellular debris and apoptotic bodies. Then, the supernatant was transferred to a new tube to perform an ultracentrifugation at 100,000 x *g* for 90 min. The vesicles were collected together with the protein aggregates in the final UC pellet. An SEC column was used to separate the compounds according to their size and remove the aggregates (**Figure 1**). In order to confirm the isolation of EVs, each SEC fraction followed a nanoparticle tracking analysis (**Figure 2A**).

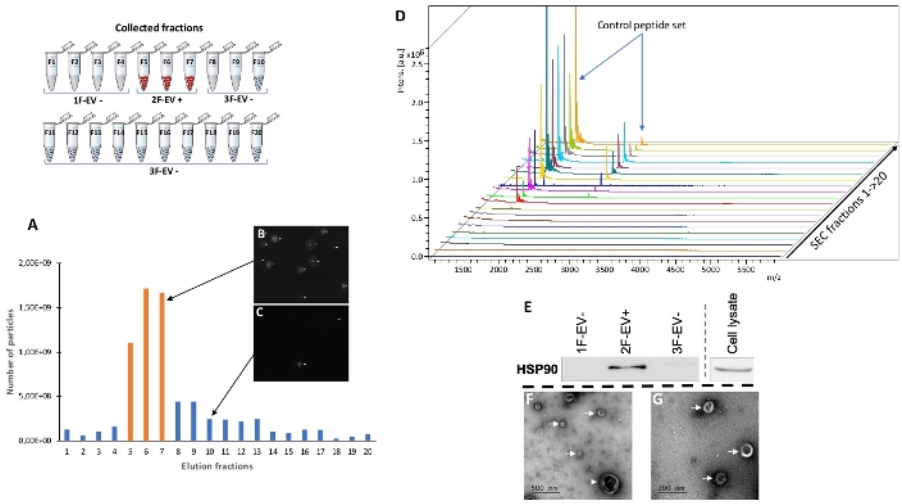


**Figure 2: Analysis of the SEC fractions.** (**A**) Nanoparticle tracking analysis (NTA) of SEC fractions. The total number of particles in each SEC fraction is presented with bar charts. The orange bar charts show the three consecutive EV+ fractions (F5–F7). (**B**, **C**) Screen captures of NTA chamber show significant differences in particle flow between SEC fractions. (**D**) Complementary MALDI mass spectrometry analysis. From another UC pellet containing EVs, a standard control peptide set was added before SEC separation in order to validate the performance of the SEC strategy. Each SEC fraction was analyzed with matrix assisted laser desorption ionization - time of flight (MALDI-TOF) to determine standard-positive fractions. In the nine first spectra (fractions 1 to 9), no signal was observed. The detection of these free standards was possible in the following fractions (fractions 10 to 20) confirming the ability of SEC procedure to separate EVs (F5–F7) from soluble components (F10–F20). (**E**) Western blot analysis of SEC fractions as an EV marker preliminary analysis. The EV+ fractions (F5–F7) were pooled as one sample (2F-VE+) whereas the EV- fractions (F1–F4 and F8–F20 respectively) were pooled in two other samples called 1F-EV- and 3F-EV-. The results showed the presence of a Heat-Shock Protein 90 (HSP90) (EV positive marker) signal in 2F-EV+, and also in cell lysate as positive control, compared to the other fractions (1F-EV- and 3F-EV-). (**F**, **G**) Electron microscopy analysis of the EV positive sample (2F-EV+). The observation under two successive magnifications revealed the presence of EVs in a size range around 100 nm (white arrows) and around 400 nm (arrowhead). Please click here to view a larger version of this figure.

The particle number was significantly higher in the fractions 5, 6 and 7 than in the previous (F1–F4) and following ones (F8–F20). It was possible to see a particle flow in these fractions even if a few particle were observed in the following fractions (**Figure 2B,C**). This separation does not prevent the possibility that fractions other than F5–F7 may contain a small amount of vesicles, or even that EV-rich fractions F5 to F7 may contain molecular contaminants. To at least ensure that the F5–F7 fractions are free of contaminating co-eluting molecules, it was necessary to follow the time-course elution of the different compounds in the SEC procedure. To do so, control peptide standards were added to a similar UC pellet as previously used. This preparation was again separated using the SEC procedure. Then, a matrix assisted laser desorption ionization — time of flight (MALDI) mass spectrometry analysis was performed in order to identify the SEC fractions in which standards were eluted (**Figure 2D**). Due to the mass range, only ionized products from peptide standards were followed in this analysis. The results showed that these products were detectable in the fractions 10 to 20, demonstrating that any soluble protein cannot be eluted in the same fractions as the EVs (F5–F7). These results confirmed the interest of this approach in the separation of EVs from non-EV components. Even assuming that the F8–F20 fractions could contain a residual fraction of EVs, we decided in the following experiments to combine the EV positive fractions (F5–F7) in a single sample called 2F-EV+. We also combined the other SEC fractions into two samples called 1F-EV- (F1–F4) and 3F-EV- (F8–F20). We grouped in three samples for several reasons. First, the number of SEC fractions would increase the time of molecular analyses but also functional in vitro studies. The EV-positive SEC fractions separately exhibit lower particle numbers and also compromise the detection of molecular compounds. In the same way, it was considered more judicious to group the fractions F8–F20 to concentrate, if necessary, the residual vesicles and check their presence by a preliminary western blot analysis against HSP90, an EV marker. Interestingly, a positive signal for HSP90 was detected in the fraction 2F-EV+, also in the cell lysate as positive control, but not in 1F-EV- and 3F-EV- samples (**Figure 2E** and **Supplementary Figure S1** as control). This analysis confirms the interest of 2F-EV+ only and the correct management of the previous SEC fractions. To affirm EV isolation, an additional experiment using electron microscopy analyzed only the 2F-EV+ sample and allowed the observation of EVs with a typical morphology and size heterogeneity between 100 and 400 nm (**Figure 2F,G**).

Another key step in the validation was proteomic analysis (**Figure 3**). We developed a whole mass spectrometry analysis with multiple objectives: (i) confirm the isolation of EVs with the detection of a high number of EV markers in 2F-EV+, (ii) eventually identify contaminant proteins in the EV negative samples (1F-EV- and 3F-EV-) and (iii) characterize the protein contents of EVs supporting their biological activities.

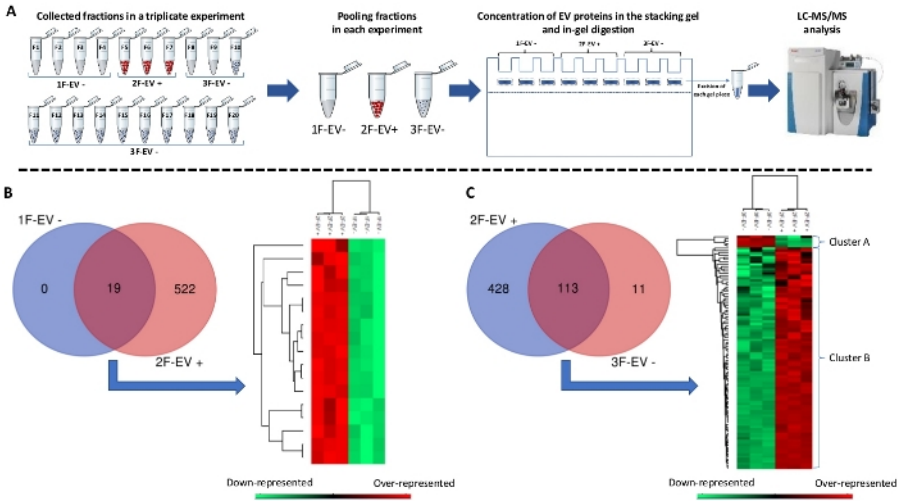


**Figure 3: Proteomic analysis of EV-positive and EV-negative samples.** (**A**) After three independent EV isolations from similar microglia cell preparations, the samples 1F-EV-, 2F-EV+ and 3F-EV- were loaded for sodium dodecyl sulfate polyacrylamide gel electrophoresis (SDS-PAGE) and migrated until the stacking gel to concentrate proteins in order to realize their in-gel digestion. The resulting peptides were then analyzed by liquid chromatography tandem mass spectrometry (LC-MS/MS) to identify the corresponding proteins. (**B**) Comparison of identified proteins between samples 1F-EV- and 2F-EV+ showing common proteins in both fractions (19) and proteins exclusively detected in the 2F-EV+ fraction (522). The heatmap shows the relative representation where all common proteins between 1F-EV- and 2F-EV+ triplicates were over-represented (red) in the 2F-EV+ samples. (**C**) Comparison of identified proteins between fractions 2F-EV+ and 3F-EV- showing common proteins between triplicates (113) and exclusively represented proteins (428 in 2F-EV+ and 11 in 3F-EV-). The heatmap shows the relative representation in two clusters. One (cluster A) presents 5 over-represented proteins in 3F-EV- sample and a second (cluster B) presents 108 over-represented proteins in 2F-EV+. Please click here to view a larger version of this figure.

From cell-conditioned media, the UC and SEC procedure led to three samples 1F-EV-, 2F-EV+ and 3F-EV-. The corresponding proteins were extracted and concentrated by sodium dodecyl sulfate polyacrylamide gel electrophoresis (SDS-PAGE). After a short migration in the stacking gel, the samples were collected by a band excision, transferred in distinct tubes to be in-gel digested. The products were separated by online reversed-phase chromatography directly coupled to a mass spectrometer for analysis (**Figure 3A**).

The following results, as an example of the whole procedure, were obtained from microglia-conditioned medium after a 48 h culture. The raw data were submitted to a Rat protein database. The identified proteins were compared between samples 1F-EV- and 2F-EV+ (**Figure 3B**) and between samples 2F-EV+ and 3F-EV- (**Figure 3C**). In the first comparison, the Venn diagram showed 19 common proteins in both fractions and 522 proteins exclusively detected in the 2F-EV+ fraction. The analysis using a quantitative proteomics software allowed the identification of the relative representation of the common proteins. The results showed a heatmap where all common proteins between 1F-EV- and 2F-EV+ triplicates were over-represented (red) in the 2F-EV+ samples. In the second comparison between fractions 2F-EV+ and 3F-EV-, 113 common proteins were identified between triplicates. Moreover, 428 proteins were exclusively detected in 2F-EV+ and 11 proteins were exclusively found in 3F-EV-. Following the quantitative analysis, the heatmap representation of the 113 common proteins highlighted two clusters where the cluster A presented five over-represented proteins in 3F-EV- sample and the cluster B presented 108 over-represented proteins in 2F-EV+.

The 428 proteins exclusively represented and the 108 proteins over-represented in 2F-EV+ were submitted to the Exocarta open access database in order to detect EV-associated molecules. The analysis of the top 100 EV markers in Exocarta highlighted the presence of 86 EV-associated proteins in 2F-EV+ (**Figure 4A**).

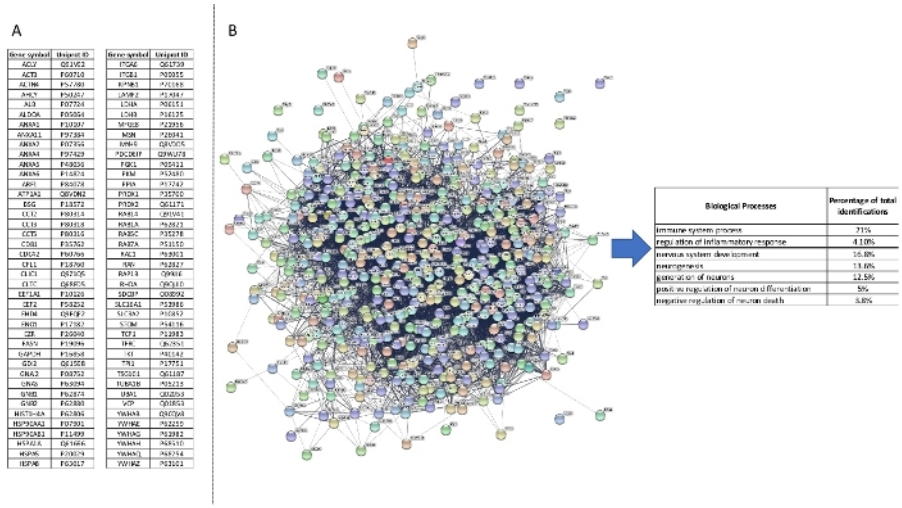


**Figure 4: Analysis of proteins from the 2F-EV+ sample.** (**A**) A pool of 536 proteins (428 exclusive and 108 over-represented proteins) was submitted to the Exocarta database in order to detect EV-associated molecules. Molecule symbols of the 86 EV-associated proteins detected in the top 100 EV markers from Exocarta database. (**B**) The prediction of protein interactions and their association to selected biological processes showed immune and neuroprotective pathways in the 2F-EV+ sample. Please click here to view a larger version of this figure.

Interestingly, the analysis of the 5 common proteins in the cluster A and the 11 proteins exclusively represented in 3F-EV- were not associated to any EV marker (data not shown). Finally, the prediction of protein interactions and their association with selected biological processes showed the presence in the 2F-EV+ fraction of immune mediators (21%) sometimes involved in the control of the inflammatory response (4.1%) (**Figure 4B**). The EV contents in 2F-EV+ were also associated with the neuronal development (16.8%), neuron differentiation (5%) and the control of neuronal death (3.8%) which is in accordance with the following neurite outgrowth assay.

Thus, the strategy that we selected makes possible the access of all data and allows a prediction of the EV-mediated functions prior to the biological assays that we then performed (**Figure 5**).

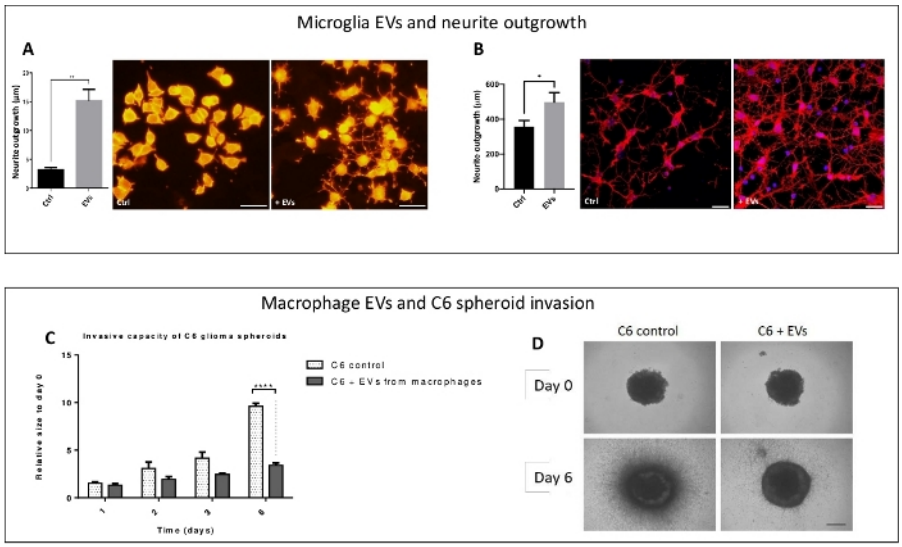


**Figure 5: EV-dependent f unctional assays.** The effects of microglia-derived EVs were evaluated on neurite outgrowth (upper frame) and the effects of macrophage-derived EVs were evaluated on glioma cell invasion (lower frame). (**A**, **B**) The neurite length was measured on PC-12 cells (Panel A was modified from Raffo-Romero et al.[16] with permission) or rat primary neurons (B). The results showed a significant outgrowth increase under EVs (+ EVs) compared to control (Ctrl). Scale bar = 20 µm. (**C**, **D**) Time course of C6 glioma spheroid invasion into collagen in the presence of rat primary macrophage-derived EVs (C6 + EVs) or vehicle (C6 control). The C6 spheroid 3D invasion into collagen was monitored and quantified up to 6 days. Quantification of tumor cell invasion are shown at 1, 2, 3 or 6 days (C) as observed on representative images (D). Scale bar = 500 µm. For neurite outgrowth assays, the significance was calculated by unpaired Student's *t*-test (* $p < 0.05$, ** $p < 0.01$ and *** $p < 0.001$). For invasion assay, the significance was calculated by one-way ANOVA followed by Tukey's post hoc test. The error bars indicate relative standard error of three independent experiments. Please click here to view a larger version of this figure.

In this way, the neurotrophic functions of microglia-derived EVs were studied on PC-12 cell line and rat primary neurons. The results showed a positive effect on the neurite outgrowth (**Figure 5A,B**). The presence of EVs respectively increased about 6 and 1.5 fold the neurite network in length and/or in number in PC-12 and primary neurons compared to a control condition. In another context, we also studied the effects of macrophage-derived EVs on a brain tumor invasion (**Figure 5C,D**). It was assessed using 3D tumor spheroids embedded in a matrix of collagen. Spheroids generated with C6 rat glioma cells were cultured for 6 days in a collagen matrix containing (or not containing) EVs purified from rat

macrophages culture medium. The collagen matrix provides a structure into which tumor cells can invade and spread out of the spheroid. The macrophage-derived EVs impaired the growth and invasion of the glioma spheroids. After a 6 day culture, a 50% decrease of the invasion was observed in EV-treated spheroids compared to the control. This result showed that macrophages can produce EVs with anti-tumoral and/or anti-invasive factors affecting the glioma growth.

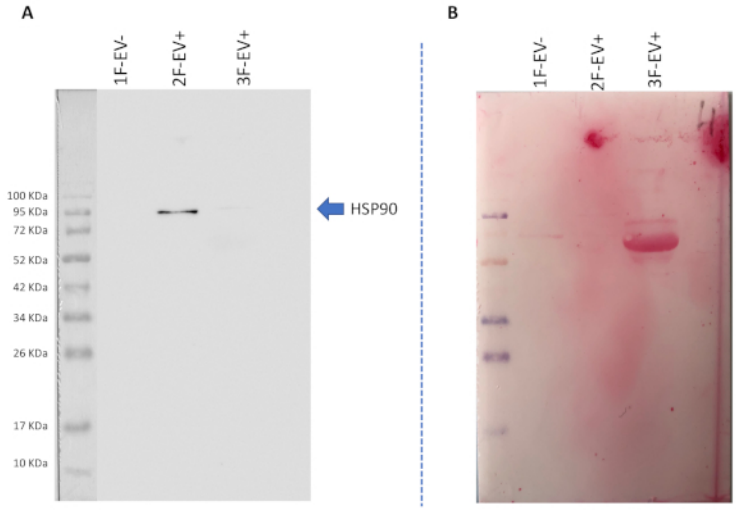


**Supplementary Figure S1: Images of membrane used for western-blotting experiment.** (**A**) Original image of the western blot from **Figure 2E** (against HSP90 EV marker). (**B**) Ponceau staining image of the same membrane showing the correct loading of protein extracts from 1F-EV-, 2F-EV+ and 3F-EV- samples. Please click here to download this figure.

## Discussion

The central nervous system (CNS) is a complex tissue in which cell-to-cell communication regulates normal neuronal functions necessary for homeostasis[30]. EVs are now widely studied and described as important molecular cargos for cell-to-cell communication[31]. They specifically deliver a cocktail of mediators to recipient cells thereby affecting their functions in healthy and pathological conditions[32]. Recent studies indicate that EVs play a crucial role in the CNS[24,33,34] and especially those from brain immune cells[35,36]. The balance between pro- and anti-inflammatory immune responses is crucial and allows maintaining the brain integrity during the synaptic development and the neuronal activities throughout life. Two distinct situations of immune responses were discussed in this study: the relationship (i) between microglia and neurons and (ii) between infiltrating macrophages and glioma cells. First, microglia are the resident macrophages in the brain tissue where they play a key immune role in the management of the microenvironment changes in order to ensure the neuronal activities. But excessive pro-inflammatory mechanisms can be supported by over-activated microglia and lead to neurodegenerative disorders[37,38]. In contrast, the high-grade gliomas require anti-inflammatory profiles and involve tumor-associated macrophages (TAMs) recruited in the tumor site. The bone marrow-derived macrophages (BMDMs) represent a large population of these TAMs in close relation with glioma cells. Under the influence of the tumor, BMDMs exhibit in vivo anti-inflammatory and pro-tumoral profiles[39]. How these BMDMs could control in vitro tumoral cell invasion is a crucial question in this report. That is why, the macrophage-derived EVs were used alone in the glioma spheroid invasion assay. Together in co-culture, the glioma cells would have influenced the macrophages to produce other EV populations with anti-inflammatory profiles. The direct use of immune EVs could be much better as anti-tumoral agent. Consequently, immune cells maintain cell-to-cell communication in specific microenvironments where the inflammatory balance is strongly influenced by external signals[40,41]. The understanding of the EV-mediated immune responses represents a great challenge to limit the pathogenesis of many disorders. The identification of biologically active EV contents is one key to understand dysregulated inflammatory processes and propose new therapeutic strategies[42,43].

In this study we present a methodology consisting in a differential ultracentrifugation process as the first step to eliminate the cell debris, the apoptotic bodies and the soluble molecules, combined with size exclusion chromatography to isolate EVs from molecular aggregates. When the EV populations are evaluated in biological assays, it is crucial to discriminate the EV contents from other co-isolated materials. That is why we improved the isolation in order to separate EV- from non EV-associated compounds. By adding standard proteins in control samples submitted to the SEC procedure, we were then able to localize their elution fractions by MALDI-TOF. Because the standards are free molecules, they globally co-elute with sample-associated molecular aggregates related to non EV materials. Thus, the EV fractions from experimental samples were validated in a reliable isolation procedure. In addition, we developed a double proteomic analysis strategy. Except the use of the anti-HSP90 antibody by western blotting as a EV marker preliminary detection, we decided to validate the correct EV fractionation by a non-targeted detection of EV-associated protein signatures. Indeed, the present approach was not deliberately focused on the detection of multiple known EV markers because of the insufficient specificity and sensitivity of certain antibodies. The variability and the abundance of some EV markers at the surface of EV subpopulations are still controversial in the isolation procedures. Moreover, an antibody-based methodology could represent a limit in a high number of organisms due to a lack of commercial antibodies while the EV studies are now a hot topic in biology. This non-targeted analysis allowed the identification of a higher number of molecules which are already described as EV markers (86 proteins in the top 100 EV markers from Exocarta database). Finally, this approach could be really useful to validate the EV isolation from poorly described organisms provided that the detected proteins could present significant homologies to known EV markers. As recently described, a large-scale proteomic analysis could be an alternative to using only a few arbitrary markers[43]. This would improve the discrimination of EV+ fractions and the identification of their active contents prior to use in biological assays.

Indeed, it is necessary to associate the characterization of EV contents to the effects that were observed in biological assays. Indeed, the biological impact of EVs to recipient cells suggests vesicular mediators or effectors to be involved. Again, the same non-targeted analysis allows the identification of biologically active molecules. A possible optimization in this analysis concerns the types of molecules it is possible to identify. Our strategy was based on the large-scale analysis of protein signatures and led to predictive biological pathways associated to immune response and neuron survival. It is essential to consider the other molecule families including lipids, mRNA and microRNAs for example. Our current studies associate these additional identifications to the protein signatures in order to get a global knowledge of this EV-dependent communication.

Many therapeutic approaches are envisaged in the coming years. Given that the EVs are able to easily cross the blood brain barrier and reach the pathological tissues, these molecular cargos can be used in different ways. Though this study did not highlight the EV surface molecules, their identification is still necessary in order to better understand the addressing process towards target cells and tissues. The proteomic analysis in our methodology gives access to these data. Otherwise, in this report, we presented the in vitro production of EVs as beneficial cocktails. We did not optimize the best conditions to prime or activate the immune cells beforehand. This point is crucial because, in the tissues, the microenvironment has a direct impact on the immune cells and ultimately contributes to shaping the biogenesis of their EVs. In the case of glioblastoma for example, it has been found that the cancer cells produce their own EVs, thus contributing to orientate the neighboring TAMs towards anti-inflammatory profiles and their local immunosuppression[44,45]. This is the reason why the macrophage-derived EVs in the glioma environment are different from those produced in a single macrophage culture. Thus, we directly used macrophage-derived EVs, separately produced from a single macrophage culture, to control the glioma spheroid invasion because a macrophage-glioma co-culture has no control on the tumor growth. Further therapeutic strategies could prevent this in vivo immunosuppression by using pro-inflammatory and anti-tumoral EVs produced in vitro from activated macrophages. A similar strategy could be used in the context of neurodegenerative diseases through the use of EVs derived from microglia properly alerted to produce a neuroprotective and anti-inflammatory response favoring the neuronal survival. In conclusion, the studies of the EV-mediated communication between immune cells and the in vivo microenvironment are key to allowing a better understanding of pathogenesis and designing innovative therapeutic approaches.

## Disclosures

The authors have nothing to disclose.

## Acknowledgments

The presented work was supported by the Ministère de L'Education Nationale, de L'Enseignement Supérieur et de la Recherche and INSERM. We gratefully acknowledge the BICeL- Campus Scientific City Facility for access to instruments and technical advices. We gratefully acknowledge Jean-Pascal Gimeno, Soulaimane Aboulouard and Isabelle Fournier for the Mass spectrometry assistance. We gratefully acknowledge Tanina Arab, Christelle van Camp, Francoise le Marrec-Croq, Jacopo Vizioli and Pierre-Eric Sautière for their strong contribution to the scientific and technical developments.

## References

1. Thion, M.S., Ginhoux, F., Garel, S. Microglia and early brain development: An intimate journey. *Science.* **362** (6411), 185–189 (2018).
2. Ginhoux, F. et al. Fate mapping analysis reveals that adult microglia derive from primitive macrophages. *Science (New York, N.Y.).* **330** (6005), 841–5 (2010).
3. Sankowski, R., Mader, S., Valdes-Ferrer, S.I. Systemic Inflammation and the Brain: Novel Roles of Genetic, Molecular, and Environmental Cues as Drivers of Neurodegeneration. *Frontiers in Cellular Neuroscience.* **9** (2015).
4. Chakrabarty, S., Kabekkodu, S.P., Singh, R.P., Thangaraj, K., Singh, K.K., Satyamoorthy, K. Microglia in health and disease. *Cold Spring Harb. Perspect. Biol.* **43** (3), 25–29 (2015).
5. Sankowski, R., Mader, S., Valdés-Ferrer, S.I. Systemic inflammation and the brain: novel roles of genetic, molecular, and environmental cues as drivers of neurodegeneration. *Frontiers in cellular neuroscience.* **9**, 28 (2015).
6. Engelhardt, B., Vajkoczy, P., Weller, R.O. The movers and shapers in immune privilege of the CNS. *Nature Immunology.* **18** (2), 123–131 (2017).
7. Louveau, A. et al. Structural and functional features of central nervous system lymphatic vessels. *Nature.* **523** (7560), 337–341 (2015).
8. Domingues, P. et al. Tumor infiltrating immune cells in gliomas and meningiomas. *Brain, Behavior, and Immunity.* **53**, 1–15 (2016).
9. Hambardzumyan, D., Gutmann, D.H., Kettenmann, H. The role of microglia and macrophages in glioma maintenance and progression. *Nature Neuroscience.* **19** (1), 20–27 (2016).
10. Thion, M.S. et al. Microbiome Influences Prenatal and Adult Microglia in a Sex-Specific Manner. *Cell.* **172** (3), 500-516.e16 (2018).
11. Hammond, T.R. et al. Single-Cell RNA Sequencing of Microglia throughout the Mouse Lifespan and in the Injured Brain Reveals Complex Cell-State Changes. *Immunity.* **50** (1), 253-271.e6 (2019).
12. Rajendran, L. et al. Emerging Roles of Extracellular Vesicles in the Nervous System. *The Journal of Neuroscience.* **34** (46), 15482–15489 (2014).
13. Gupta, A., Pulliam, L. Exosomes as mediators of neuroinflammation. *Journal of Neuroinflammation.* **11** (1), 68 (2014).
14. van Niel, G., D'Angelo, G., Raposo, G. Shedding light on the cell biology of extracellular vesicles. *Nature Reviews Molecular Cell Biology.* **19** (4), 213–228 (2018).
15. Budnik, V., Ruiz-cañada, C., Wendler, F. Extracellular vesicles round off communication in the nervous system. *Nature Reviews Neurosciences.* **17** (March), 160–172 (2016).
16. Raffo-Romero, A. et al. Medicinal Leech CNS as a Model for Exosome Studies in the Crosstalk between Microglia and Neurons. *International Journal of Molecular Sciences.* **19** (12), 4124 (2018).
17. Zhou, Y. et al. Exosomes Transfer Among Different Species Cells and Mediating miRNAs Delivery. *Journal of Cellular Biochemistry.* **118** (12), 4267–4274 (2017).

 

18. Arab, T. et al. Proteomic characterisation of leech microglia extracellular vesicles (EVs): comparison between differential ultracentrifugation and Optiprep™ density gradient isolation. *Journal of extracellular vesicles.* **8** (1), 1603048 (2019).
19. Murgoci, A.-N. et al. Brain-Cortex Microglia-Derived Exosomes: Nanoparticles for Glioma Therapy. *ChemPhysChem.* **19** (10), 1205–1214 (2018).
20. Glebov, K. et al. Serotonin stimulates secretion of exosomes from microglia cells. *Glia.* **63** (4), 626–634 (2015).
21. Hooper, C. et al. Wnt3a induces exosome secretion from primary cultured rat microglia. *BMC Neuroscience.* **13** (1), 144 (2012).
22. Gabrielli, M. et al. Active endocannabinoids are secreted on extracellular membrane vesicles. *EMBO reports.* **16** (2), 213–220 (2015).
23. Antonucci, F. et al. Microvesicles released from microglia stimulate synaptic activity via enhanced sphingolipid metabolism. *The EMBO Journal.* **31** (5), 1231–1240 (2012).
24. Frühbeis, C., Fröhlich, D., Kuo, W.P., Krämer-Albers, E.-M. Extracellular vesicles as mediators of neuron-glia communication. *Frontiers in Cellular Neuroscience.* **7**, 182 (2013).
25. Prada, I. et al. Glia-to-neuron transfer of miRNAs via extracellular vesicles: a new mechanism underlying inflammation-induced synaptic alterations. *Acta neuropathologica.* **135** (4), 529–550 (2018).
26. Takenouchi, T. et al. Extracellular ATP induces unconventional release of glyceraldehyde-3-phosphate dehydrogenase from microglial cells. *Immunology Letters.* **167** (2), 116–124 (2015).
27. Yang, Y., Boza-Serrano, A., Dunning, C.J.R., Clausen, B.H., Lambertsen, K.L., Deierborg, T. Inflammation leads to distinct populations of extracellular vesicles from microglia. *Journal of Neuroinflammation.* **15** (1), 168 (2018).
28. Duhamel, M. et al. Paclitaxel Treatment and Proprotein Convertase 1/3 (PC1/3) Knockdown in Macrophages is a Promising Antiglioma Strategy as Revealed by Proteomics and Cytotoxicity Studies. *Molecular & Cellular Proteomics.* **17** (6), 1126–1143 (2018).
29. Pool, M., Thiemann, J., Bar-Or, A., Fournier, A.E. NeuriteTracer: A novel ImageJ plugin for automated quantification of neurite outgrowth. *Journal of Neuroscience Methods.* **168** (1), 134–139 (2008).
30. Domingues, H.S., Portugal, C.C., Socodato, R., Relvas, J.B. Oligodendrocyte, Astrocyte, and Microglia Crosstalk in Myelin Development, Damage, and Repair. *Frontiers in Cell and Developmental Biology.* **4**, 71 (2016).
31. Rashed, M.H. et al. Exosomes: From Garbage Bins to Promising Therapeutic Targets. *Int. J. Mol. Sci. Int. J. Mol. Sci.* **18** (18) (2017).
32. Yuana, Y., Sturk, A., Nieuwland, R. Extracellular vesicles in physiological and pathological conditions. *Blood Reviews.* **27** (1), 31–39 (2013).
33. Frohlich, D. et al. Multifaceted effects of oligodendroglial exosomes on neurons: impact on neuronal firing rate, signal transduction and gene regulation. *Philosophical Transactions of the Royal Society B: Biological Sciences.* **369** (1652), 20130510–20130510 (2014).
34. Krämer-Albers, E.-M. et al. Oligodendrocytes secrete exosomes containing major myelin and stress-protective proteins: Trophic support for axons? *Proteomics. Clinical applications.* **1** (11), 1446–61 (2007).
35. Verderio, C. et al. Myeloid microvesicles are a marker and therapeutic target for neuroinflammation. *Annals of Neurology.* **72** (4), 610–624 (2012).
36. Prada, I., Furlan, R., Matteoli, M., Verderio, C. Classical and Unconventional Pathways of Vesicular Release in Microglia. *GLIA.* **61**, 1003–1017 (2013).
37. Prinz, M., Priller, J. The role of peripheral immune cells in the CNS in steady state and disease. *Nature Neuroscience.* **20** (2), 136–144 (2017).
38. Li, Q., Barres, B.A. Microglia and macrophages in brain homeostasis and disease. *Nature Reviews Immunology.* (2017).
39. Kennedy, B.C. et al. Tumor-Associated Macrophages in Glioma: Friend or Foe? *Journal of Oncology.* **2013**, 1–11 (2013).
40. Ilaria, Potolicchio., Gregory, J. Carven., Xiaonan, Xu., Christopher, Stipp, Richiard, J. Riese., Lawrence, J. Stern, and Santambroggio, L. Proteomic Analysis of Microglia-Derived Exosomes: Metabolic Role of the Aminopeptidase CD13 in Neuropeptide Catabolism1. *The Journal of Immunology.* **175**, 2237–2243 (2005).
41. Turola, E., Furlan, R., Bianco, F., Matteoli, M., Verderio, C. Microglial microvesicle secretion and intercellular signaling. *Frontiers in Physiology.* **3 MAY** (2012).
42. Cocucci, E., Meldolesi, J. Ectosomes and exosomes : shedding the confusion between extracellular vesicles. *Trends in Cell Biology.* **25** (6), 364–372 (2015).
43. Théry, C. et al. Minimal information for studies of extracellular vesicles 2018 (MISEV2018): a position statement of the International Society for Extracellular Vesicles and update of the MISEV2014 guidelines. *Journal of Extracellular Vesicles.* **7** (1), 1535750 (2018).
44. de Vrij, J. et al. Glioblastoma-derived extracellular vesicles modify the phenotype of monocytic cells. *International Journal of Cancer.* **137** (7), 1630–1642 (2015).
45. van der Vos, K.E. et al. Directly visualized glioblastoma-derived extracellular vesicles transfer RNA to microglia/macrophages in the brain. *Neuro-Oncology.* **18** (1), 58–69 (2016).


 